



IDENTIFICATION OF THE DISPERSOID IN A Mg-Al-Y ALLOY

W.J. Park and Nack J. Kim

Center for Advanced Aerospace Materials
Pohang University of Science and Technology
San 31, Hyojadong, Pohang 790-784 Korea

(Received October 29, 1994)

(Revised November 29, 1994)

Introduction

In recent years, there has been a growing interest in the Mg alloys for structural applications because of their low density. Although the advantages which can be offered by low density Mg alloys are quite obvious, the alloys have so far been used for few applications, mostly in non-critical components. There are several factors which limit the structural application of Mg alloys, namely, low strength, poor ductility and poor corrosion resistance. It has been recently shown that the application of rapid solidification for the Mg alloys has resulted in a significant improvement in mechanical properties and corrosion resistance. Rapid solidification extends the solid solubility limits, allowing the addition of novel alloying elements in larger contents than for ingot casting without gross segregation, and results in a refinement of microstructures and the formation of new or metastable phases which are beneficial to the properties. For example, in rapidly solidified Si containing Mg alloys, it has been observed that fine Mg_2Si dispersoids, formed in as-rapidly solidified ribbons, do not coarsen appreciably during high temperature consolidation and are quite effective in pinning the grain boundaries [1,2]. As a result, some of the rapidly solidified Mg-Si based alloys exhibit good combinations of strength and ductility. Greater improvement in mechanical properties and corrosion resistance has been obtained by adding Y and/or other rare earth alloying elements to Mg-Al alloys [2-6]. A yield strength of 460 MPa with total elongation of 5% and good corrosion resistance (corrosion rate of 0.28 mm/yr. in a 3% NaCl solution) was reported for a Y containing Mg-Al alloy [4]. Improvement in properties of Y containing Mg alloys is believed to be due to the fine grain size and the presence of fine dispersoids in the microstructure. Despite the importance of the fine dispersoid present in an Mg-Al alloy, however, its nature is not yet clear. This dispersoid shows a very high thermal stability at elevated temperatures, which is not expected from Mg-Y or Mg-Al-Y intermetallic compounds. The present study is aimed at characterizing the dispersoid present in a rapidly solidified Mg-Al alloy containing Y. An ingot cast alloy of the same composition has also been examined to highlight the similarities and differences between rapidly solidified and conventionally processed alloys. The main techniques used for this investigation were analytical electron microscopy techniques, in particular, convergent beam electron diffraction (CBED) and energy dispersive X-ray spectroscopy (EDS).

Experimental

A pre-alloyed Mg-5Al (wt.%) ingot and elemental Y were melted in a stainless steel crucible at 950°C and were melt spun into thin ribbons (25 to 50 μm thickness). An alloy of the same composition was also ingot

cast using a chill casting technique. Thin foils for transmission electron microscopy were prepared by ion beam thinning. Microstructural characterization of the samples was performed at an operating voltage of 120kV.

Results and Discussion

Rapidly Solidified Alloy

Figure 1a shows the typical microstructure observed in the thin foils made from the rapidly solidified Mg-5Al-6Y alloy ribbon. There is a fine dispersion of second phase particles (about 20 nm in diameter) within the Mg matrix. Selected area diffraction (SAD) patterns do not show any diffraction spots other than those of the Mg matrix; instead they are mostly composed of ring patterns (Figure 1b). Some of these ring patterns matched with those for MgO. This is undoubtedly due to the presence of MgO on the surface of TEM foil due to rapid oxidation. Besides ring patterns from MgO, there are a couple of ring patterns, arising from the dispersoids present in the Mg matrix. However, these ring patterns are incomplete and thus, positive identification of dispersoids cannot be made. Moreover, SAD ring patterns obtained from these dispersoids cannot be indexed as any of the known Mg or Mg/Al containing phases.

EDS microanalysis of the dispersoid shows that it contains Mg, Al and Y, while the matrix contains Mg (Figure 2). The fine size of the dispersoid makes the quantitative compositional analysis difficult mainly because of the interaction with the surrounding matrix. It is quite possible that some of the spectra obtained from dispersoid invariably comes from the surrounding matrix. To obtain a true chemistry of the dispersoid, the foil thickness was measured using the contamination-spot-separation method [7] and the matrix X-ray spectrum was differentiated from that of the dispersoid. The effect of beam broadening was also considered and corrected by means of Monte Carlo simulation [8]. Using a measured foil thickness of 129 nm and assuming that the dispersoid is spherical ($d = 20$ nm) and sits at the middle of the foil, we find that among the elements detectable by EDS, only Al and Y are present in significant quantities in the dispersoid, with the ratio of Al to Y in the range 2:1 to 3:1. There are a large number of possible phases which contain Al and Y, e.g., (1) if the dispersoid contains O, then YAG, and similar compounds could form. and (2) if the dispersoid is an intermetallic phase, then Al_2Y , Al_3Y , and such intermetallics could form. The presence of O or the other light

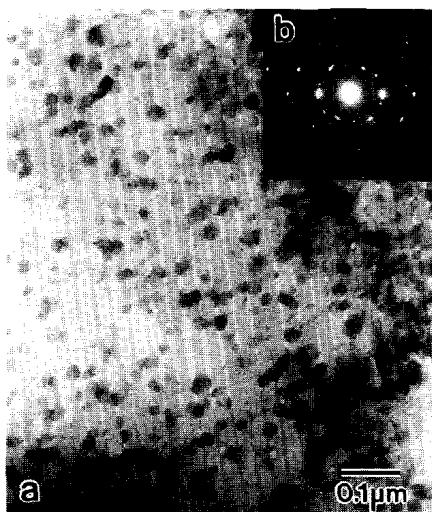


Figure 1. a) BF micrograph of the as-rapidly solidified Mg-5Al-6Y alloy ribbon and b) SAD pattern.

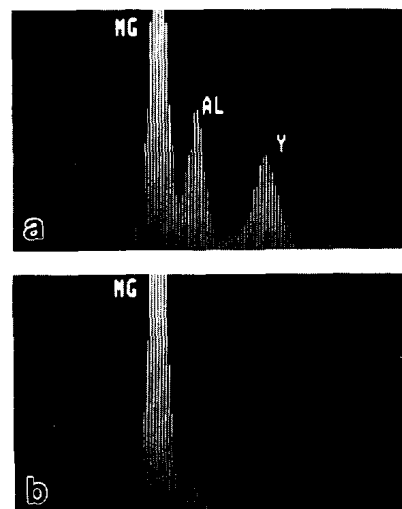


Figure 2. EDS spectra obtained (a) the dispersoid and (b) the matrix.

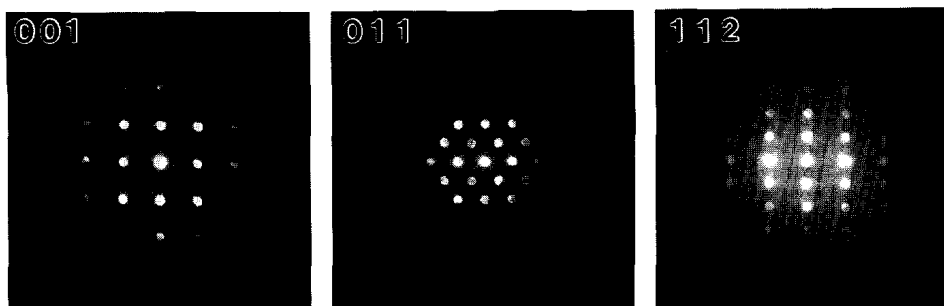


Figure 3. CBED patterns of the Al_2Y dispersoid in rapidly solidified alloy.

elements could not be verified due to the unavailability of light element detectors; however, if one assumes that the dispersoid is intermetallic (does not contain O or other light elements), then the composition of the dispersoid is close to Al_2Y or Al_3Y .

CBED studies were attempted to obtain electron diffraction information for the dispersoids (Figure 3). Although it does not show the details of the crystallographic information due to the extremely fine dispersoid size, analysis of the patterns shows that the patterns agree with those of Al_2Y . In fact, a couple of unidentified ring patterns shown in Figure 1 can be indexed based on the structure of Al_2Y .

Ingot Cast Alloy

As has been shown above, the dispersoid present in the rapidly solidified alloy is extremely fine, which makes the unambiguous identification of the dispersoid difficult. To complement the information obtained from the rapidly solidified alloy, an alloy with the same composition as that for the rapidly solidified alloy was chill cast and its microstructure was characterized. Two types of particles have been identified in the microstructure of the ingot cast alloy: 1) $\text{Mg}_{17}\text{Al}_{12}$ phase in the form of platelets and 2) an Al and Y containing phase in the form of blocky particles whose size ranges from 2 to 4 μm .

Identification of the Al and Y containing phase was again conducted by using the techniques of CBED and EDS. Based on the quantitative analysis of the EDS spectra, the chemical composition of the phase can be suggested to be Al_2Y , in agreement with the result obtained in the rapidly solidified alloy. Examples of CBED patterns obtained from the Al and Y containing phase are shown in Figure 4. The crystal point group of a phase can be determined by analyzing the pattern symmetries in the bright field 000 reflection and the whole pattern including the higher order Laue zone (HOLZ) of CBED patterns using the method of Buxton et al. [9]. Not all of the CBED patterns show the presence of HOLZ lines in 000 discs; in such cases, the diffraction group can be deduced from projection diffraction symmetries. As shown in Figure 4, the projection diffraction and whole pattern symmetries are both 4mm for the [001] orientation, which places the diffraction group as 4mm or $4\text{mm}1_{\text{r}}$. For the [011] zone axis, the projection diffraction and whole pattern symmetries are both 2mm, which give 2mm or $2\text{mm}1_{\text{r}}$ as the diffraction group. For the [111] zone axis, bright field and whole pattern symmetries are both 3m, placing the diffraction group as 3m or $6_{\text{r}}\text{mm}_{\text{r}}$. For the [013] zone axis, bright field and whole pattern symmetries are both m, which gives the diffraction group as m or $2_{\text{r}}\text{mm}_{\text{r}}$. The possible point groups corresponding to the above diffraction groups are summarized in Table 1. From Table 1, it can be established that the point group of the dispersoids is $m\bar{3}m$. After identifying the point group of the dispersoid, the next step required for deducing its space group is identification of its Bravais lattice. The Bravais lattice of a phase can be deduced by examining the spacings and positions of reflections in the zero order Laue zone (ZOLZ) and the first order Laue zone (FOLZ). Measurement of spacings of the ZOLZ and FOLZ from the pattern (zone axis [111]) in Figure 4 gives $d_{\text{FOLZ}}/d_{\text{ZOLZ}} = 2$, which agrees with the value for the face-centered or diamond cubic structures.

Point group $m\bar{3}m$ gives the several possible space groups such as $Pm\bar{3}m$, $Pn\bar{3}n$, $Pm\bar{3}n$, $Pn\bar{3}m$, $Fm\bar{3}m$, $Fm\bar{3}c$, $Fd\bar{3}m$, $Fd\bar{3}c$, $Im\bar{3}m$ and $Ia\bar{3}d$. Face-centered or diamond cubic structure of the dispersoids leaves the $Fm\bar{3}m$, $Fm\bar{3}c$, $Fd\bar{3}m$ or $Fd\bar{3}c$ as the possible space group for the dispersoids. Further analysis of the space group can be performed by analyzing the dynamic absences present in some of the CBED patterns. However, the dynamic absences are not observed in any of the patterns in the present case, so it is not possible to determine the space group of dispersoids by analyzing the dynamic absences. Close examination of the d-spacings obtained from the [001] CBED pattern, however, shows that the (200) type reflections are absent, limiting the space group to be $Fd\bar{3}m$ or $Fd\bar{3}c$. In the space group $Fd\bar{3}c$, reflections of type hhl, for which $h+l = 2n$, are forbidden [10]. All of the CBED diffraction patterns show these reflections except (200) type, indicating that the correct space group of the dispersoid is $Fd\bar{3}m$. By measuring the spacings of the discs in various diffraction patterns, the lattice parameter of the dispersoids has been found to be $a = 0.786$ nm. By comparing the space group, lattice parameter and EDS information obtained above with the information given in Powder Diffraction File [11], the nature of the dispersoid can unambiguously be identified as Al_2Y .

Concluding Remarks

The second phase present in the rapidly solidified Mg-Al-Y alloy has been shown to be identical in structure to a second phase detected in the ingot cast alloy. Although the cooling rates achieved with rapid solidification is high enough to induce the formation of metastable or nonequilibrium phases in most cases, the observation that the Al_2Y phase has formed in both the rapidly solidified alloy and the ingot cast alloy indicates that the formation of nonequilibrium Al_2Y phase is not necessarily due to rapid solidification. Nevertheless, the benefits of rapid solidification have been demonstrated in that the rapidly solidified alloy has a much finer, more uniform dispersion of Al_2Y phase than the ingot cast alloy. The origin of Al_2Y in this alloy system can be understood by considering the melting procedures. For the melting of the desired alloy composition, prealloyed Mg-5Al (wt.%) and elemental Nd have been added to the crucible and melted at 950°C . Although the Mg and Al both have low melting points (648.8°C and 660.37°C , respectively), it is not expected that Y which has a high melting point (1523°C) will melt at 950°C . In this case, it is quite possible that a reaction between Y and other alloying elements may occur during melting, forming a Y containing intermetallic compound. It has been shown that, in the present case, Y reacts with Al to form Al_2Y . Similar behavior has been found in several Mg alloy systems, e.g., AZ91 alloy with the addition of MN [12], Mg-Al alloy with the addition of Zr and Ce [13], and more recently, Nd containing Mg-Al-Zn alloy [14].

The presence of "insoluble" Al_2Y in the Mg alloys imparts significant advantages over other more conventional Mg alloys. Such a dispersoid would have only a small tendency to coarsen and would, therefore, retain much of its beneficial effects even after prolonged exposure to high temperature.

TABLE 1
Possible Point Groups Corresponding to Deduced Diffraction Groups

Diffraction Group	Possible Point Groups
$4mm$	$4mm$
$4mm1_2$	$4/mmm$ $m\bar{3}m$
$2mm$	$mm2$ $\bar{6}m$ $\bar{6}m2$
$2mm1_2$	mmm $4/mmm$ $6/mmm$ $m\bar{3}$ $m\bar{3}m$
$3m$	$3m$ $\bar{4}3m$
6_2mm_2	$\bar{3}m$ $m\bar{3}m$
m	m $mm2$ $4mm$ $\bar{4}2m$ $3m$ $\bar{6}$ $6mm$ $\bar{6}m2$ $\bar{4}3m$
2_2mm_2	$2/m$ mmm $4/m$ $4/mmm$ $\bar{3}m$ $6/m$ $6/mmm$ $m\bar{3}$ $m\bar{3}m$

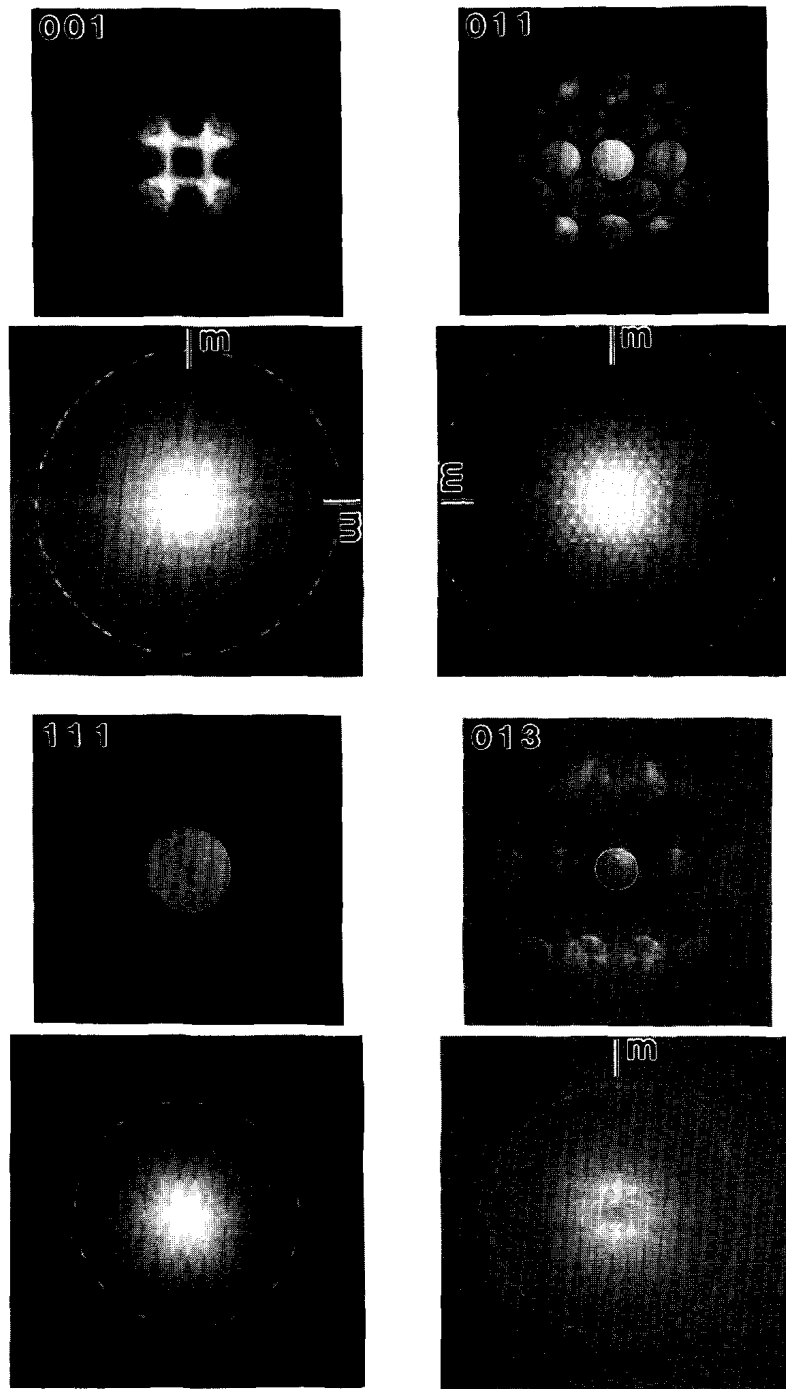


Figure 4. CBED patterns of the Al_2Y dispersoid in the ingot cast alloy.

Acknowledgments

This work was supported by the Korea Science and Engineering Foundation.

References

1. S. K. Das and C. F. Chang, in *Rapidly Solidified Crystalline Alloys*, eds., S. K. Das, B. H. Kear and C. M. Adam, TMS-AIME, Warrendale, PA, 137 (1985).
2. H. Gjestland, G. Nussbaum and G. Regazzoni, in *Light Weight Alloys for Aerospace Applications*, eds., E. W. Lee, E. H. Chia and N. J. Kim, TMS, Warrendale, PA, 139 (1989).
3. C. F. Chang, S. K. Das and D. Raybould, in *Rapidly Solidified Materials*, eds., P. W. Lee and R. S. Carbonara, ASM, Metals Park, OH, 129 (1986).
4. C. F. Chang, S. K. Das, D. Raybould and A. Brown, *Metal Powder Report*, 41(4), p. 302 (1986).
5. C. F. Chang, S. K. Das, D. Raybould, R. L. Bye and N. J. Kim, in *Space Age Metals Technology*, eds., F. H. Froes and R. A. Cull, SAMPE, Covina, CA, 345 (1988).
6. G. Nussbaum, G. Regazzoni and H. Gjestland, in *Science and Engineering of Light Metals*, eds., K. Hirano, H. Oikawa and K. Ikeda, The Japan Institute of Light Metals, Tokyo, 115 (1991).
7. G. W. Lorimer, G. Cliff and J. N. Clark, in *Developments in Electron Microscopy and Analysis*, ed., J. A. Venables, The Academic Press, London, 153 (1976).
8. D. F. Kyser, in *Introduction to Analytical Electron Microscopy*, eds., J. J. Hren, J. I. Goldstein and D. C. Joy, Plenum Press, New York, 199 (1976).
9. B. F. Buxton, J. A. Eades, J. W. Steeds and G. M. Rackham, *Phil. Trans. Roy. Soc., London*, A281, 171 (1976).
10. *International Tables for Crystallography*, ed., T. Hahn, D. Reidel Publishing Co., Dordrecht, Holland, A604 (1984).
11. *Powder Diffraction File*, International Center for Diffraction Data, Swarthmore, PA (1989).
12. H. A. Robinson and P. F. George, *Corrosion*, 10, 182 (1954).
13. R. S. Busk and T. I. Leontis, *Trans. AIME.*, 188(2), 297 (1950).
14. W. J. Park, H. Park, D. H. Kim and Nack J. Kim, *Materials Science & Engineering*, A179/A180, 637 (1994).